JOURNAL OF SOLID STATE CHEMISTRY 72, 193–200 (1988)

Determination of Lithium Sites within the Possible Fast Ion Transport Ceramic $Li_2O : 14Nb_2O_5$ by High-Resolution Electron Microscopy

B. M. GATEHOUSE

Department of Chemistry, Monash University, Clayton 3168, Australia

AND P. GOODMAN AND A. OLSEN*

Division of Materials Science and Technology, CSIRO, Clayton 3168, Australia

Received January 26, 1987

The structure of the interstitially distributed lithium compound $Li_{5x}Nb_{2-x}O_5$ has been determined by high-resolution microscopy. Substantial agreement with the earlier X-ray diffraction determined structure was obtained with the notable exception that the symmetry is lowered from *C2/m* to *Cm*. The structure allows crystallographic orientations suitable for device construction to be predicted.

Introduction

Despite the fact that the material with the stoichiometric composition $Li_2O : 14Nb_2O_5$ was established as a stable region of the phase diagram of the LiO_2/Nb_2O_5 system by Reisman and Holtzburg in 1958 (*1*), its detailed structure has remained unknown until the present time. Crystallographic studies of the compound, a high-temperature ceramic, were first undertaken by Lundberg and Andersson (*2*) and Andersson (*3*) who showed that Li-free and Li-bearing preparations of $N–Nb_2O_5$ gave identical powder data. Andersson (*3*) made a parallel study of the Li-bearing material using the Weissenberg X-ray diffraction technique, but with a twinned crystal. The structure was found to be monoclinic with possible space groups *C2/m*, *C2*, and *Cm*, and with cell dimensions $a = 2.851$ nm, $b = 0.383$ nm, $c = 1.748$ nm, and $\beta = 120.80°$. Nb and O positions were refined within the space group *C2/m*. The sample was prepared in the presence of LiF. Since stoichiometric F did not show up in the refinement it was assumed to be absent from the structure. The fact that Li atoms were not resolved however was hardly surprising in view of their light scattering power and the lack of perfection in the crystals. More recently, Roth *et al.* (*4*) confirmed that the compound observed by Reisman and Holtzburg had systematic absences consistent with the above space groups in a survey of materials relating to fast ion transport. At this stage one of the

* Permanent address: Department of Physics, University of Oslo, Blindern, Norway.

0022-4596/88 $3.00

present authors (B.M.G.) became determined to initiate a fresh investigation, capitalizing on the techniques of "structure imaging" then being developed at Arizona State University by Cowley and Iijima (*5*). Furthermore he employed a fluorine-free technique, heating $LiCO_3$ and Nb_2O_5 in platinum at 1000°C for 71 hr with subsequent cooling over 24 hr. Since initial X-ray diffraction analysis gave the N–Nb_2O_5 structure and no additional atomic positions, a principal aim was to examine the visibility of Li by the new technique. However, the micrographs obtained at that time using the JEOL 100B electron microscope (*6*) raised more questions than were answered, since they could not be reconciled *geometrically* with the X-ray derived N–Nb_2O_5 structure (*2*). Furthermore, more recent electron microscope studies by Fung and Yang (*7*) have given essentially similar micrographs as those of (*6*). The present investigation was carried out therefore with the twofold aim of (a) resolving the existing conflict between X-ray and electron microscope evidence, and (b) determining the main Li sites with a view to predicting bulk electrolyte behavior. This type of analysis has become feasible with the advent of the JEOL 200CX microscope, with a resolution in excess of 0.2 nm.

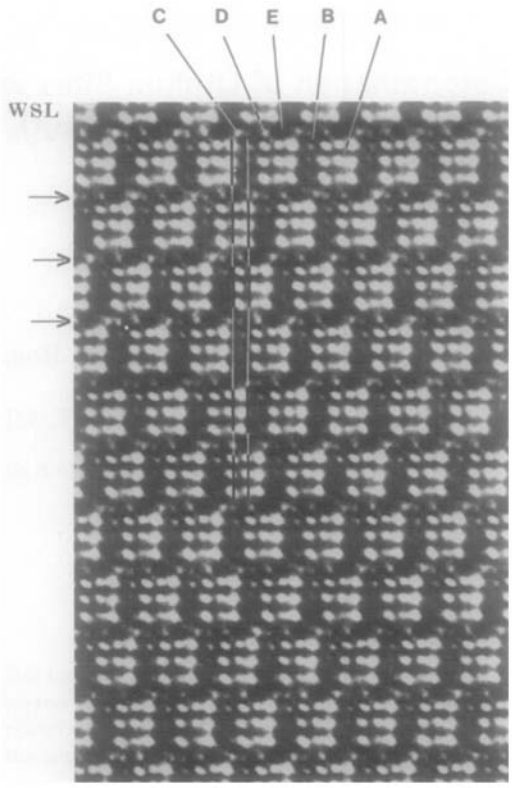

FIG. 1. High-resolution image of $Li_2O:14Nb_2O_5$ in [001] orientation. Drawn vertical lines indicate small lateral shift between imaged structural units as discussed in text; Wadsley shear lines (WSL) are similarly indicated by arrows on the left.

Experimental Results

Samples were crushed from the solid to make the electron microscope sample. Since only fine details distinguish the Li-free and Li-bearing N–Nb_2O_5 images, measurements were made using secondary ion mass spectrometry (SIMS) to confirm the presence of Li in the crystals used in the following study.

Figure 1 shows an image taken with the incident beam parallel to the [001] axis of the space group *B2/m* (second setting nomenclature: (*8*) and (*9*)), and may be compared directly with the structure of N–Nb_2O_5 drawn in that projection (*2*) (cf. Fig. 2). The main feature of Fig. 1 derives from the N–Nb_2O_5 raft structure, in which 4 × 4-unit cell blocks (infinite along the *c*-axis) of corner-sharing octahedra form a structural unit (Fig. 2). Adjacent rows of these units are separated by Wadsley shear planes, called Wadsley shear *lines* in projection, and referred to here, and in Fig. 1, as "WSL." Bright dots in the micrographs (Figs. 1 and 4) correspond to *holes* in the structure, following the "projected charge density" approximation (*10*).

On the other hand, a realistic comparison of the image of Fig. 1 with the structure of Fig. 2 requires a proper electron-optical

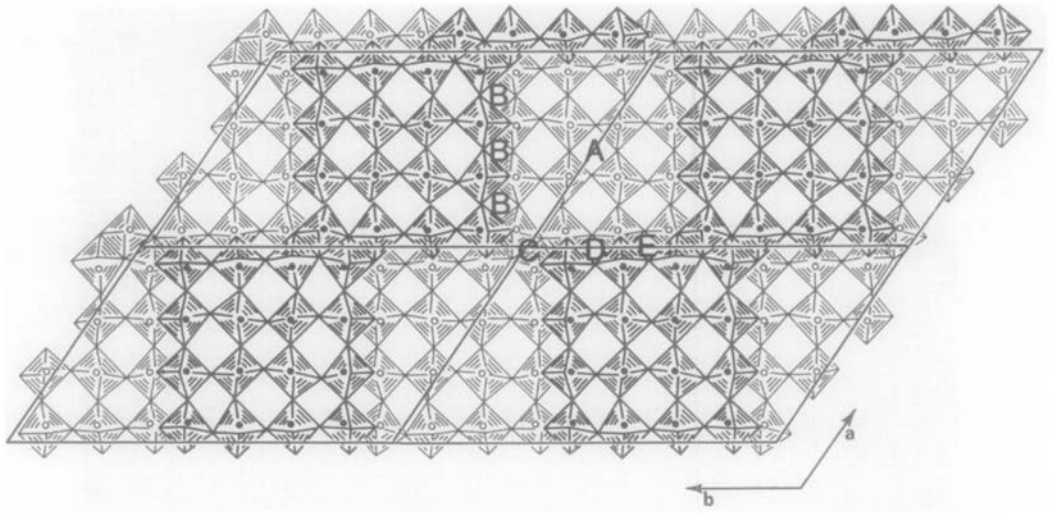

FIG. 2. Drawing of the Andersson structure of N–Nb_2O_5, in the [001] projection, given in the nomenclature of space group *B2/m*, with interstitial sites A, B, C, D, and E indicated as discussed in text.

calculation. Carrying this out using the "multi-slice" method (*11*) leads to the simulated image of Fig. 3. For this calculation a diffraction aperture of 0.5 $Å^{-1}$ was used, limiting the effective resolution in the result to 0.2 nm. This allows the 3 × 3 arrays of cubo-octahedral-sized holes—the "A" sites of Fig. 1—to be computed, but omits details smaller, in the projection of Fig. 2, than 0.2 nm, such as the holes labeled B, C, D, and E, from the image. (NOTE: all these latter sites are octahedral in three dimensions.) In this way we have omitted details from the simulated image which fall outside the well-known transfer function of the objective lens, while highlighting the electron-optical "shift" produced under practical operating conditions in the 200 CX, i.e., using a spherical aberration coefficient of 0.94 mm and a defocus of $\Delta f = -50$ nm. This shift is highlighted in Fig. 3 by vertical drawn lines passing through the center of the image holes in the first row.

Referring now to the micrograph of Fig. 1 we find that the alignment between structural "hole" images in the *x*-direction matches that displayed in Fig. 3 fairly well, i.e., there is a slight displacement of approximately one-fourth of an octahedral unit, as highlighted by drawn vertical lines. If however we were to compare either Fig. 1 or Fig. 3 with the micrograph of Fig. 4, showing the equivalent micrograph from the same preparative batch of material obtained in 1976 (*6*), we find approximately double the value of electron-optical shift between these imaged structural units occurring in the earlier micrograph (Fig. 4: with equivalent drawn lines). No equivalent simulated image has been made for this (100B) microscope in the present study since we are not sure of the appropriate lens function but it is very logical to attribute the additional shift to a larger spherical aberration and possibly larger $-\Delta f$ value. When the two micrographs are put together as in Fig. 5, casual inspection would have one believe the more contemporary micrograph (Fig. 5a) to be in close agreement with the geometric structure of Fig. 2 and the earlier one (Fig. 5b) to differ markedly, since the shift value of approximately one-

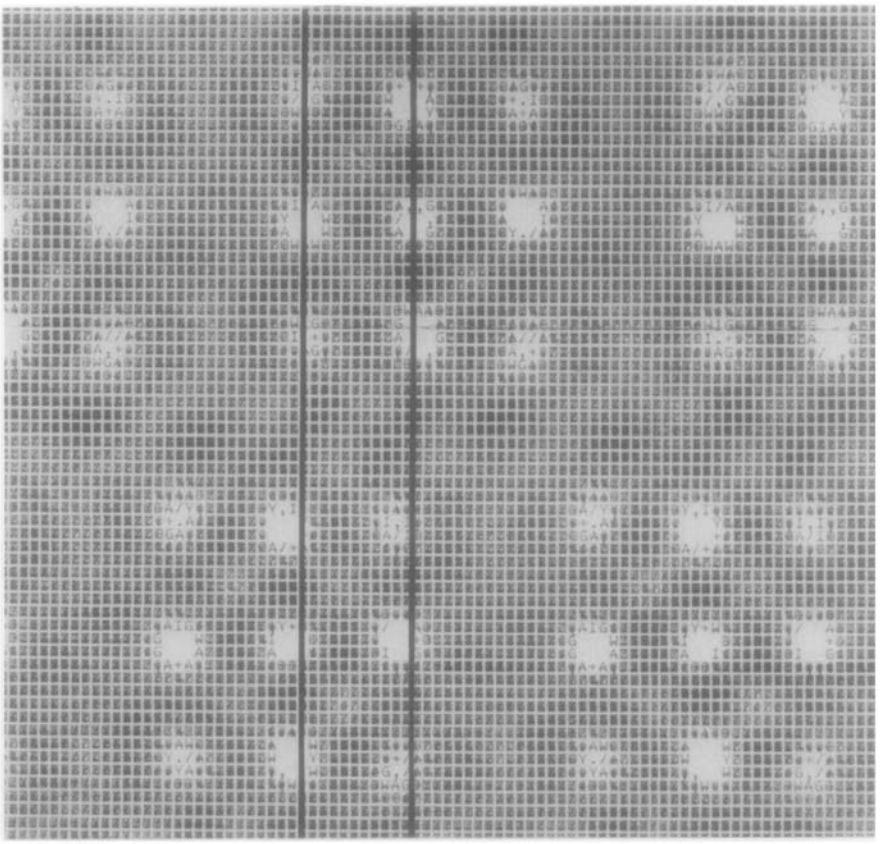

FIG. 3. Computer-simulated image for the Andersson structure, for the electron-optical conditions appropriate to Fig. 1, but with an imposed diffraction aperture of 0.5 $Å^{-1}$, with vertical lines drawn to show the computed lateral shift, displayed in Fig. 1.

half of an octahedral unit gives quite the wrong *apparent* structure. However, the whole exercise so far is an argument against the naive, or noncomputative comparison of micrograph and structural projection from a real-space three-dimensional unit cell. Lack of appreciation of this at the time (1976), in the view of the present authors, removes the former so-called discrepancy referred to in the introduction. It should be noted that the *projected space group* of the structure, N–Nb_2O_5, namely $p2$, has been retained throughout the imaging process. This occurs since the lens function, after accurate stigmation, has circular symmetry.

The next step in analysis is the interpretation of details finer than 0.2 nm in Fig. 1. Although these details are beyond sensible calculation since they fall outside that region of the lens-transfer function for the 200CX which is well established, they can nevertheless be interpreted on grounds of symmetry, since, again, the unknown but stigmated lens function at least retains circular symmetry and the space group of the framework or Li-free N–Nb_2O_5 has been established (*2*).

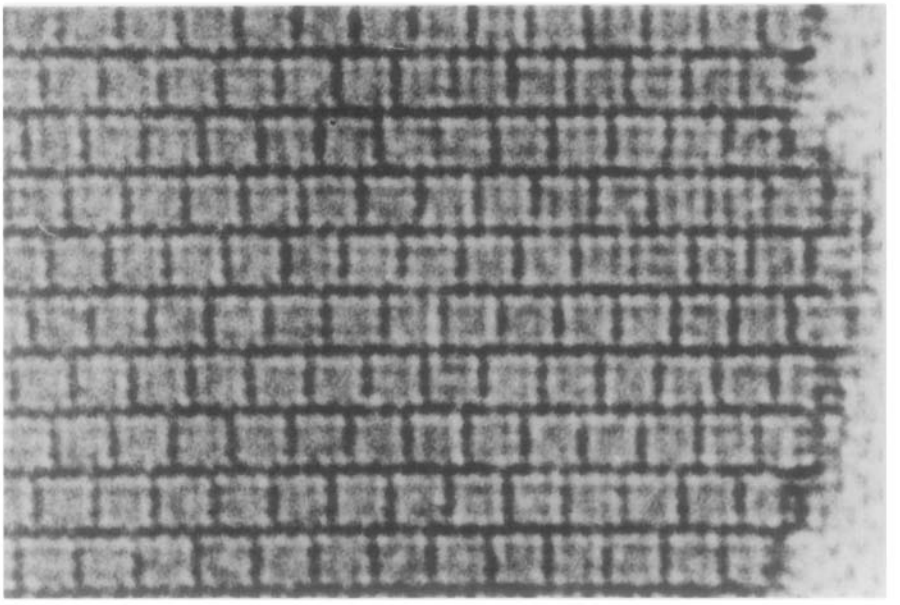

FIG. 4. Section of the 1976 JEOL 100B electron micrograph of $Li_2O:14Nb_2O_5$.

Interpretation of Image Details B, C, D, E

The variations in image detail of Fig. 1 are very obvious in the enlarged section, shown in Fig. 6. These are caused by local fracture-surface roughness, giving variable electron-optical refraction, and more importantly, by milliradian random deviations from the [001] setting arising from a slight crystal curvature. To locate subunit cell segments at the correct [001] setting for structural interpretation, areas of maximized symmetries are sought, following standard practice in this situation (e.g., (*12*)), in this case with the starting assumption of a $p2$ projection symmetry (see above). First we define the drawn symbols in Fig. 6, using the code B, C, D, E, for the

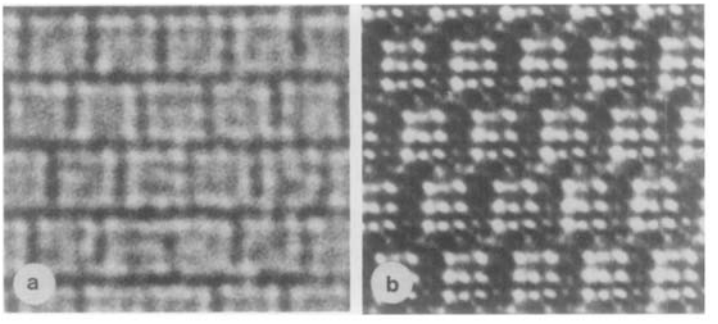

FIG. 5. Comparable segments of (a) contemporary and (b) earlier micrograph.

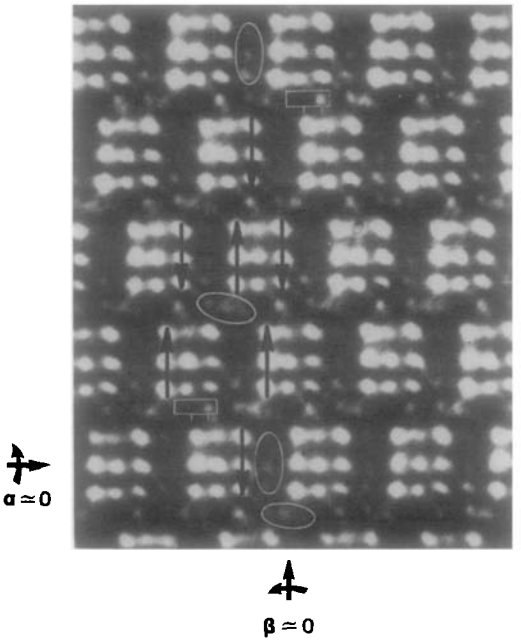

FIG. 6. Enlarged section of Fig. 1, with critical features indicated (see text).

interoctahedral sites of Fig. 2 in electron-optical image form. Thus, the (two) vertical ellipses surround the three adjacent holes B; according to $p2$ these should have a centrosymmetric form, and this is found approximately inside the *lower* ellipse, where the central hole is brightest. A second ellipse type, diagonally inclined, indicates (two) sites C, directly over the center of symmetry (a diad in projection). The image should correspondingly be symmetrical in the same regions as the triple B image, this occurs *approximately* at both the delineated sites, where a symmetrical triplet appears.

Subgroup Symmetry of $Li_2O:14Nb_2O_5$

Finally, a drawn rectangular box surrounds two of the double D–E sites of the Fig. 6 image field, with white marker lines to indicate these site positions. Throughout this field, and in fact that of Fig. 1, the asymmetry between the site D and E images is clear, despite the image irregularities discussed above, with D bright and E dark. This interpretation is aided by the drawing of Fig. 7, in which the space group symbols of $B2/m$ are drawn over the Andersson structure of Fig. 2. This observation (the inequality of D and E) means that quite certainly a structural nonequivalence between these sites, crystallographically equivalent to $p2$ symmetry, has been determined for these 200CX images of the Li-filled N–Nb_2O_5 having the formula

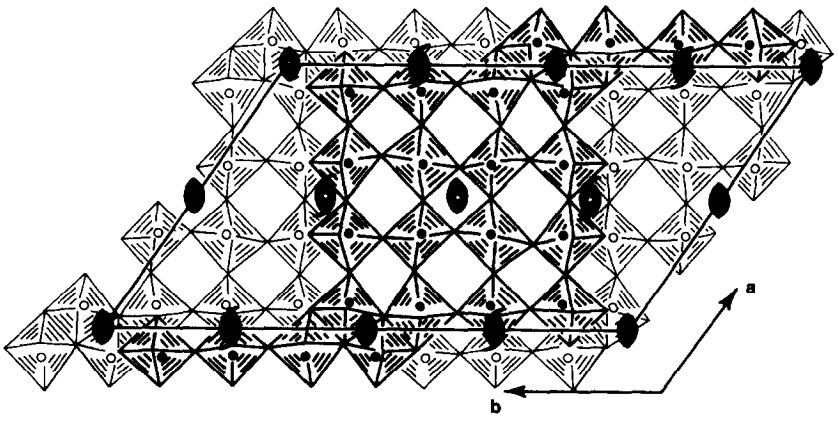

FIG. 7. Andersson structure with space group symbols added, following the space group conventions for $B2/m$ in the IUCr. tables.

$14Nb_2O_5$. The obvious interpretation of bright and dark (D and E) sites is correspondingly that of empty and partially Li-filled tunnels. Given the uncertainty in the lens function at these resolutions, the opposite coding, reversing the interpretations for D and E, is of course feasible since the lens function oscillates when central symmetry in its outer region (e.g., Fig. 13.3 of (*13*)). However, either way the *structural* interpretation, arrived at through symmetry considerations, is the same, viz., that the center of symmetry demanded by the space group *B2/m*, leading to the equivalence of sites D and E, must be broken by the alternate ordering of interstitially sited Li between these sites. The corresponding subgroup symmetry determines the three-dimensional space group as either *Cm* or *C*1. Finally, since the unit cell is only one octahedra deep (0.38 nm) we are reluctant to allow that the mirror symmetry could be lost and conclude the subgroup to be *Bm*, i.e., *Cm* in standard nomenclature.

It is noted here that convergent beam diffraction data purporting to show the existence of a vertical two-fold axis parallel to [001] in this compound was published earlier by Fung and Yang (*7*), in apparent contradiction to present findings. However, we now know that the results of convergent beam symmetry analysis cannot be transferred arbitrarily to the microscopic scale (e.g., Refs. (*14, 12*)), and find no difficulty in reconciling their data with our own.

Observability of Li in High-Resolution Images

Recently there has been some debate about the observability of Li atoms in lattice images, since this has seldom if ever been previously reported. This must be at least partly due to the fact that Li atoms occur frequently in solid solution when their detectability is not to be expected (e.g., Ref. (*15*)). There are two obvious mechanisms by which the Li sites might be detected when they are part of the periodic structure. One is the blocking effect whereby holes are filled and bright contrast becomes dark. For this effect to be important the holes need to be sufficiently small in projection, commensurate with the filling atom. The $Li_2O:14Nb_2O_5$ is favored with such Li-commensurate sites, and with an equally favored projection for this detection. The second mechanism alluded to above is the size-effect mechanism, discussed below.

Charge Balance

With the above evidence for Li incorporated interstitially into the Andersson structure (*2*), charge balance requires an electrically equivalent framework *Nb* replacement, in the ratio 1 : 5, as occurs, for example, in the *L*–$LiNb_3O_8$ structure (*16*). This would lead to a unit cell composition of $16(Li_{5x}Nb_{2-x}O_5)$. With the $Li_2O:Nb_2O_5$ ratio of 1 : 14, the x value is 0.028 and the unit cell composition $Li_{1.8}(Li_{0.45}Nb_{31.55})O_{80}$, in agreement with the proposal of Roth *et al.* (*4*). These framework-incorporated Li ions could in principle be detected by the so-called size effect mechanism, whereby a small displacement of nearest-neighbor atoms caused by the substitution is rendered "visible" in an electron microscope (*17*). However, in the present instance the data is insufficiently precise even to show that this substitution occurs, let alone to determine the substituted-site coordinates. From charge neutrality considerations we can assume at present that this does occur, and past experience with other structures (e.g., Refs. (*18, 12*)) would lead us to believe that the substitution would be quasi-periodic over several unit cells. The present space group allocation naturally ignores this possible substitutional ordering.

Conclusions

In the above analysis we determine the local space group of the ordered component of the compound to be *Cm*, and the composition to be $Li_{2.25}Nb_{31.55}O_{80}$, with Li occupation along the Wadsley shear planes ordered in alternative sites.

This location of Li atoms gives a structure consistent with existing X-ray refinement, and furthermore shows the possible mechanism of a Li-transport electrolyte. The alternative Li occupation of crystallographically equivalent N–Nb_2O_5 sites with a partial occupational density suggests that Li site hopping along these planes could occur under an external field. It can be predicted that Li-ion conductivity will be markedly anisotropic in this structure. Ion transport with an average "*c*" or *z*-direction can occur with a zigzag path without blocking; transport along the *x*-axis on the other hand is blocked by the Wadsley shear planes, and that along the *y*-axis by the large cubo-octahedral holes (corresponding to the A sites) which would act to both trap and disperse Li ions and Li-ion motion. This in turn suggests crystallographic orientations suitable for device construction.

References

1. A. Reisman and F. Holtzberg, *J. Amer. Chem. Soc.* **80,** 6503 (1958).
2. M. Lundberg and S. Andersson, *Acta Chem. Scand.* **19,** 1376 (1965).
3. S. Andersson, *Z. Anorg. Allg. Chem.* **351,** 106 (1967).
4. R. S. Roth, H. S. Parker, W. S. Brower, and J. L. Waring, *in* "Fast Ion Transport in Solids" (W. Van Gool, Ed.), p. 220, North-Holland, Amsterdam (1973).
5. J. M. Cowley and S. Iijima, *Z. Naturforsch., A* **27,** 445 (1972).
6. S. Iijima, private communication (1974).
7. K. K. Fung and C. Y. Yang, *Ultramicroscopy* **13,** 333 (1984).
8. N. F. M. Henry and K. Lonsdale, Eds., "International Tables for X-ray Crystallography," Vol. 1, Kynoch Press, Birmingham, AL (1964).
9. T. Hahn, Ed., "International Tables for Crystallography," Vol. A, Reidel, Dordrecht (1981).
10. D. F. Lynch and A. F. Moodie, *Acta Crystallogr., Sect. A* **31,** 300 (1975).
11. P. Goodman and A. F. Moodie, *Acta Crystallogr., Sect. A* **30,** 280 (1974).
12. P. Goodman, J. D. McLean, A. Olsen, and I. Wilson, "Analytical Microscopy 1984" (D. B. Williams and D. C. Joy, Eds.), San Francisco Press (1984).
13. J. M. Cowley, "Diffraction Physics," North-Holland, Amsterdam/New York (1981).
14. A. Olsen, J. D. McLean, and P. Goodman, *in* "Proceedings of the 41st Annual Meeting EMSA" (G. W. Bailey, Ed.), p. 40, San Francisco Press (1983).
15. N. Tanaka and J. M. Cowley, "Proceedings of the 42nd Annual Meeting EMSA" (G. W. Bailey, Ed.), p. 430, San Francisco Press (1984).
16. B. M. Gatehouse and P. Leverett, *Cryst. Struct. Commun.* **1,** 83 (1972).
17. P. Goodman, A. Olsen, and H. J. Whitfield, *Micron* **13,** 247 (1982).
18. P. Goodman and J. D. McLean, *Acta Crystallogr., Sect. B* **32,** 3285 (1976).